Indonesian Journal of Science & Technology

Journal homepage: http://ejournal.upi.edu/index.php/ijost/

Green Extraction of Anthocyanins from Red Dragon Fruit Peel Using Choline Chloride-Urea Deep Eutectic Solvents: A Sustainable Valorization Strategy Aligned with the Sustainable Development Goals (SDGs)

Xiaoqin Meng[1], Lee Hong Tee[2,], Abdulkareem Sh. Mahdi Al-Obaidi[1], Yin Hui Chow[1]*

[1]School of Engineering, Faculty of Innovation and Technology, Taylor's University, Malaysia
[2]School of Energy and Chemical Engineering, Xiamen University Malaysia, Malaysia
*Correspondence: E-mail: leehong.tee@xmu.edu.my

ABSTRACT

This study proposes a sustainable extraction strategy for anthocyanins from red dragon fruit peel using a choline chloride:urea (1:2) deep eutectic solvent (DES) system, contributing to the Sustainable Development Goals (SDGs), particularly SDGs 3, 9, and 12. Extraction conditions were optimized through Box-Behnken design and response surface methodology, targeting temperature (25-45 °C), phase ratio (0.5-2), and solid-liquid ratio (1:10-50 g/mL). The optimal parameters (33°C, 1:1.7 phase ratio, and 48:1 mg/mL solid–liquid ratio) achieved a 99.5% yield (29.15 mg/100 g) of total anthocyanins, outperforming conventional techniques. The FTIR confirmed the structural integrity of both DES and anthocyanins, with hydrogen bonding facilitating efficient solubilization under mild, non-degradative conditions. This environmentally friendly method transforms agricultural waste into high-value antioxidants, advancing circular bioeconomy principles. The approach offers scalable potential for application in the food, pharmaceutical, and cosmetic industries, reinforcing responsible production practices while promoting innovation in green extraction technologies.

ARTICLE INFO

Article History:
Submitted/Received 10 May 2025
First Revised 06 Jun 2025
Accepted 07 Aug 2025
First Available Online 08 Aug 2025
Publication Date 01 Dec 2025

Keyword:
Anthocyanins,
Box-behnken design,
Deep eutectic solvent,
Extraction,
Optimization,
Response surface methodology.

1. INTRODUCTION

Red dragon fruit (*Hylocereus polyrhizus*), commonly known as pitaya or pitahaya, belongs to the cactus family and is a high-value fruit widely cultivated in tropical and subtropical regions [1, 2]. According to statistics from the Food and Agriculture Organization (FAO), global production of red dragon fruit exceeded 3 million tons in 2023, with Southeast Asia and China being the main producing regions, accounting for more than 70% of the total output. However, during processing and consumption, the peel constitutes 30-40% of the total fruit weight and is typically regarded as agricultural waste-either discarded directly or utilized as low-value animal feed [3]. This not only leads to a significant waste of resources but also poses environmental risks, as the uncontrolled decomposition of organic matter can contribute to soil and water pollution, greenhouse gas emissions, and odor problems.

In recent years, with the growing emphasis on sustainable development, the concept of a circular economy has gained increasing attention. The circular economy advocates for the efficient use and reuse of resources by minimizing waste and extending product lifecycles. In this context, valorizing agricultural by-products like red dragon fruit peel is essential-not only to reduce environmental pollution but also to transform waste into value-added products, thereby promoting more sustainable agricultural and food processing systems. Among various valorization approaches, the recovery of bioactive compounds from fruit peels has emerged as a promising strategy.

Anthocyanins [4], as water-soluble flavonoid compounds, possess significant antioxidant, anti-inflammatory, and anticancer physiological functions [5]. Therefore, they hold important application value in the fields of food, medicine, and cosmetics. Research indicates that dragon fruit, particularly the skin of red dragon fruit, is rich in anthocyanins, polysaccharides, and flavonoids [6], making it a highly promising natural source of anthocyanins. However, at present, there is still room for optimization in the extraction process of anthocyanins from the peel of red dragon fruit to improve the extraction efficiency and product quality.

Currently, the extraction of dragon fruit anthocyanins mainly employs ultrasonic-assisted methods [7], organic solvent extraction methods [8], microwave-assisted extraction methods [9], and dual-enzyme-assisted extraction methods [10]. However, these methods typically rely on high energy input, expensive equipment, or toxic organic solvents, which can limit their industrial scalability and raise environmental concerns. Moreover, to date, there has been no report on the use of green solvents with low toxicity and high efficiency for the extraction of dragon fruit anthocyanins [11].

Traditional extraction methods, such as soaking and hot reflux, though simple to operate, have significant drawbacks, including long extraction times, large solvent consumption, and low extraction efficiencies. In recent years, ultrasonic-assisted extraction (UAE) has attracted attention due to its ability to shorten extraction time and increase yield [12]. Technologies such as microwave-assisted extraction (MAE) and enzyme-assisted extraction have also shown promising prospects [13]. However, these approaches heavily depend on specialized instruments and considerable energy consumption, which are not always accessible in small- or medium-scale production settings. Therefore, it is essential to explore environmentally friendly solvents that can replace traditional organic solvents and reduce energy consumption, enabling the chemical industry to move toward greener and more sustainable processes [14, 15]. Deep eutectic solvents (DES), as a class of green solvents, have garnered significant attention due to their low toxicity, biodegradability, and excellent solubilizing ability for various bioactive compounds [16]. Despite their potential, existing research on DES-based anthocyanin extraction has mostly focused on combining DES with external forces such

DOI: https://doi.org/10.17509/ijost.v10i3.88934
p- ISSN 2528-1410 e- ISSN 2527-8045

as ultrasound or microwave, and systematic studies on direct extraction using DES alone are extremely limited.

Considering these gaps, developing a simple, efficient, and low-energy-consumption extraction strategy using DES without complex auxiliary measures could greatly simplify the extraction process and reduce costs, providing a breakthrough direction for theoretical and applied research in anthocyanin extraction.

DES are formed by combining hydrogen bond acceptors (HBAs) such as choline chloride with hydrogen bond donors (HBDs) like urea, sugars, amino acids, or organic acids, resulting in eutectic mixtures with melting points much lower than their components [13, 17]. The simplicity of preparation, the wide availability of raw materials, and the tunable physicochemical properties make DES an attractive option for industrial applications. Compared to conventional organic solvents, DES offers several advantages, including negligible volatility, reduced flammability, and excellent solubilization capacity for a variety of bioactive compounds. These features not only minimize environmental and safety concerns but also enable DES to achieve comparable or superior extraction yields in many cases [18]. Therefore, DES holds significant potential as a sustainable alternative to traditional solvents for extracting valuable phytochemicals from plant matrices, with broad applications in the food, cosmetic, and pharmaceutical industries.

Aqueous two-phase systems (ATPS) offer an efficient and eco-friendly platform for purifying polyphenolic compounds [19], leveraging the spontaneous formation of two immiscible aqueous phases when two water-soluble components surpass critical concentrations. Although traditionally reliant on polymer-salt mixtures (widely applied in protein purification), modern ATPS development emphasizes green solvents like DES for bioactive extraction [19]. Studies consistently validate this approach. Demonstrations include a DES-ATPS yielding flavonoids from mulberry leaves with an extraction efficiency of 95.6%, demonstrating the method's high selectivity and effectiveness [20].

This study aims to develop an environmentally friendly, low-energy extraction strategy for anthocyanins from red dragon fruit peel using a DES-aqueous two-phase system (DES-ATPS), without the need for ultrasound, microwave, or enzymatic assistance. The novelty of this research lies in the direct use of a choline chloride–urea (1:2) DES system to efficiently extract and stabilize anthocyanins under ambient conditions, achieving high yield and selectivity while maintaining compound integrity. Unlike previous studies that relied on assisted extraction, this work demonstrates that DES alone, when properly optimized using response surface methodology, can achieve superior performance with enhanced environmental compatibility. The findings contribute to Sustainable Development Goals (SDGs), particularly SDG 3 (Good Health and Well-being) by promoting natural antioxidants, SDG 9 (Industry, Innovation and Infrastructure) through the development of green processing technologies, and SDG 12 (Responsible Consumption and Production) by valorizing agricultural waste into high-value bioactive compounds.

2. METHODS

This study employed the DES-ATPS to extract anthocyanins from the red dragon fruit peel, utilizing Box-Behnken response surface design (BBD) and response surface optimization extraction processes. This study aims to improve the efficient extraction process of dragon fruit anthocyanins, enhance the high added value of red dragon fruit peel, and provide a reference for the comprehensive utilization of red dragon fruit in the field of functional foods.

DOI: https://doi.org/10.17509/ijost.v10i3.88934
p- ISSN 2528-1410 e- ISSN 2527-8045

DES-based ATPS for the extraction of anthocyanins, as shown in **Figure 1**. Detailed information is explained in the next subsections.

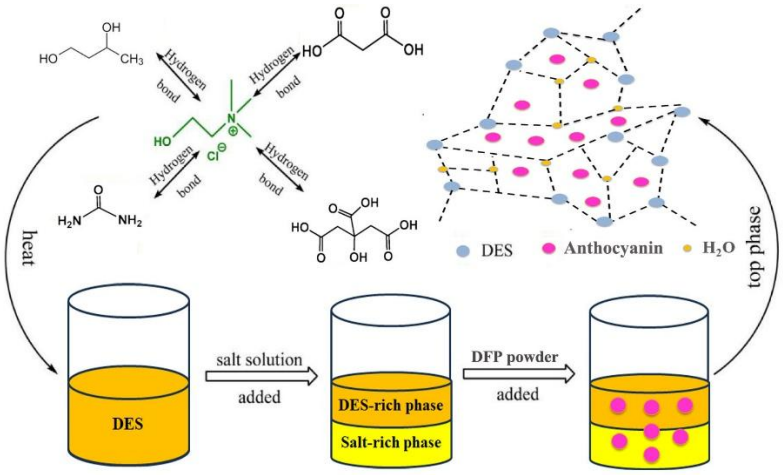

Figure 1. DES-based ATPS for the extraction of anthocyanins.

2.1. Red Dragon Fruit Material

Red dragon fruit used were collected from a local shop in Chow Kit market, Kuala Lumpur, Malaysia, and the peels of the fruits were removed, washed with distilled water, and chopped into 1 cm^2 pieces using a stainless steel knife. These pieces were put into the refrigerator, freeze-dried at -20°C for 24 hours [21]. Then, dried at -100°C for 48 hours by freeze dryer. To ensure that the dragon fruit peel powder is fully dissolved in the DES-ATPS solution, the dried pieces are ground into powder in a laboratory dry blender and sieved through an 800 µm-mesh sieve. Defatting of dragon fruit peel is carried out to prevent the interference of lipophilic nutrients with the analysis that will be carried out. The dry powder underwent defatting using hexane (AR grade) to remove the oil and dried at room temperature, then dried (room temperature drying then 24 hours in the oven to obtain a fine powder, stored in the refrigerator before use [22].

2.2. Chemical and Reagents

Choline chloride (AR grade) was purchased from Chemiz, while 1,2-Butanediol (98%) was purchased from Sigma-Aldrich (Japan). On the other hand, 1,3-Butanediol (AR grade) and 1,4-Butanediol (AR grade) were purchased from Merck (Germany). Dipotassium Phosphate (AR grade) and Ethanol (95%) were purchased from Fisher Scientific (United Kingdom) and Friendemann Schmidt Chemical, respectively. Urea (AR grade) and other chemicals were purchased from ChemSoln. The water utilized in all experiments underwent purification via a reverse osmosis system apparatus (Vexer, Smart VOS 106). Further details regarding the mentioned materials can be found in **Table 1**.

Table 1. Sources and purity of the materials.

Materials	Purpose of use
Choline Chloride (≥98%, AR grade) Urea (AR grade) 1,2-Butanediol (1,2-BDO) (AR grade) 1,3-Butanediol (1,3-BDO) (AR grade) 1,4-Butanediol (1,4-BDO) (AR grade) Dipotassium Phosphate (AR grade) Potassium Dihydrogen Phosphate (AR grade)	Preparation and Screening of DES-ATPS

DOI: https://doi.org/10.17509/ijost.v10i3.88934
p- ISSN 2528-1410 e- ISSN 2527-8045

Table 1 (continue). Sources and purity of the materials.

Materials	Purpose of use
Hexane (AR grade)	Defatting
Folin-Ciocalteu Reagent (AR grade)	TPC
NaCl (AR grade)	
Gallic Acid (AR grade)	
$NaNO_2$ (AR grade)	TFC
$AlCl_3$ (AR grade)	
NaOH (AR grade)	
Ethanol (≥99.9%)	
Quercetin (AR grade)	
Bovine Serum Albumin (BSA) (AR grade)	Protein
Bradford Dye (AR grade)	
DPPH (1,1-diphenyl-2-picrylhydrazyl) (AR grade)	DPPH
Butylated Hydroxytoluene (BHT) (AR grade)	
Methanol (HPLC grade)	
ABTS (2,2-Azino-bis-3-ethylbenzothiazoline-6-sulfonic acid) (AR grade)	ABTS
Ascorbic Acid (AR grade)	
Ethanol (AR grade)	
Sulfuric Acid (95-98%) (AR grade)	Sugar
Anthrone (AR grade)	
Sodium Dihydrogen Phosphate Monohydrate (AR grade)	Extraction
Nylon Syringe Filter	Filtration

2.3. Extraction Procedures

The anthocyanin extraction procedure was performed following the method described by other study [6], with slight modifications.

According to the set conditions, varying amounts of dragon fruit peel powder (50 mg, 150 mg, and 250 mg) were dissolved in a DES-ATPS extraction system composed of ChCl: Urea (1:2)/ ChCl: 1,2-BDO (1:4)/ ChCl: 1,3-BDO (1:4)/ ChCl: 1,4-BDO (1:4) and K_2HPO_4 with varying two-phase volume ratios, respectively.

We weighed and mixed with the DES-ATPS solution in a beaker. The mixture was stirred at 500 rpm for approximately 10 minutes. After the anthocyanin extraction, the solution was transferred into 15 mL graduated centrifuge tubes, thoroughly mixed using a vortex mixer, and then centrifuged at 6000 rpm for 10 minutes to facilitate phase separation. The top and bottom phases were carefully collected using a micropipette. Both phases were analyzed for total anthocyanin content (TAC), total betalain content (TBC), total phenolic content (TPC), total sugars (TSC), and further characterized by high-performance liquid chromatography (HPLC). Each extraction condition was conducted in triplicate to ensure reproducibility. The extraction procedures are illustrated in **Figure 2**.

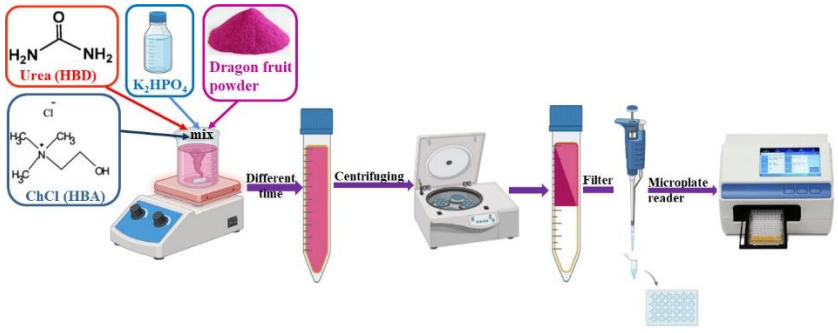

Figure 2. Schematic diagram of the extraction procedures.

DOI: https://doi.org/10.17509/ijost.v10i3.88934
p- ISSN 2528-1410 e- ISSN 2527-8045

2.4. Pre-Screening

Based on the preliminary study on screening suitable ChCl-based DES-ATPS systems, four DES-ATPS systems were selected for further investigation in this study. These include ChCl-1,2 BDO (1:4), ChCl-1,3 BDO (1:4), ChCl-1,4 BDO (1:4), and ChCl-Urea (1:2), each combined with K_2HPO_4 salt solution. These systems were chosen as the extraction systems for the current optimization study. This study systematically evaluated the performance of the four DES-ATPS formulations by comparing multiple characterization indicators. Key parameters such as antioxidant capacity (DPPH, ABTS), TAC, TBC, total flavonoid content (TFC), TPC, and TSC were thoroughly analyzed. The purpose of the pre-screening step was to establish a comprehensive evaluation system for assessing the extraction performance of DES-ATPS, to identify the most suitable DES-ATPS formulation for bioactive compound extraction, and to provide a theoretical basis for improving process parameters and enhancing the separation efficiency of bioactive substances.

2.4.1. Determination of antioxidant capacity

Several determinations are in the following:

(i) Determination of 1,1-diphenyl-2-picryl hydrazyl (DPPH) free radical scavenging activities. The method of [23] was adapted to determine the DPPH (1,1-diphenyl-2-picrylhydrazyl) free radical scavenging activities of the extract. Specifically, 1.74 g of DPPH powder is added to 25 mL of ethanol which gives 0.2 mM of DPPH reagent, an aliquot of 100 µL sample or butylated hydroxytoluene (BHT) at varying concentrations (20-100 µg/mL) was mixed with 900 µL of 0.2 mM DPPH solution prepared in methanol and was left to react for 30 min in the dark at room temperature. The absorbance reading was then taken at the wavelength of 515 nm against a blank using the microplate reader. Absorbance of a control, containing only 0.2 mM DPPH solution, was measured. The percentage (%) of DPPH radical scavenging activity was calculated. Data were presented as IC50 values for each sample. IC50 is the concentration of sample or standard (BHT) that inhibits 50% of the DPPH radicals in l µg/mL.

(ii) Determination of 2,2-Azino-bis-3-ethylbenzothiazoline-6-sulfonic acid (ABTS) free radical scavenging activities. The extraction and determination of 2,2-Azino-bis-3-ethylbenzothiazoline-6-sulfonic acid (ABTS) free radical scavenging activities was carried out using the method described by [24]. The ABTS dye was made by mixing 5 mL ABTS solution (7 mmol/L) with 88 µL of potassium persulfate solution (140 mM) and a 16-hour dark incubation of the mixture at room temperature. Then, an initial absorbance (0.7 at 734 nm) of the prepared ABTS+ solution was obtained by diluting with analytical grade ethanol. After that, a dragon fruit sample of 10 µL was added to a 96-well plate together with previously prepared diluted ABTS solution of 290 µL, followed by a 6-minute dark incubation at room temperature. The absorbance was measured at 734 nm wavelength, and the standard curve of absorbance versus weight of ascorbic acid (5-100 µg/mL) was plotted. The ABTS results were calculated based on the standard curve and expressed as mg of ascorbic acid equivalents per gram (mg AAE/g) of dry weight samples.

2.4.2. Determination of total anthocyanin content (TAC)

The extraction and determination of total anthocyanin content were carried out using the method described by [24], with slight modifications. Take 200 µL of the top and lower phases after extraction in section 2.3, dilute them to 600 µL with ultrapure water, and mix thoroughly

DOI: https://doi.org/10.17509/ijost.v10i3.88934
p- ISSN 2528-1410 e- ISSN 2527-8045

using a vortex mixer. Then, take 300 µL of the diluted solution and measure it using a Microplate Reader (BMG Labtech/Spectro star nano) at the maximum wavelength of 535 nm (distilled water as the zero blank); the analyses were carried out in triplicate. The total anthocyanin content (TAC) is expressed in milligrams of cyanidin-3-glucoside equivalents per 100 grams of sample. It is calculated using Eq. (1).

$$TAC\ \left(\frac{mg}{100g}\right) = \frac{A \times MW \times DF}{\varepsilon \times l} \times 100 \quad (1)$$

Where, *A* is the absorbance; MW is the molecular weight of cyanidin-3-glucose (449.2 g/mol); DF is the dilution factor; Ɛ is the molar absorptivity (26,900 L/mol), and *l* is the length of the cell (1 cm).

2.4.3. Determination of total betacyanin content (TBC)

The betacyanins concentration of the samples was quantified using a Microplate Reader (BMG Labtech). All the samples were subjected to 3× Dilution with distilled water, followed by taking the measurements at the maximum wavelength of 538 nm for each sample. The measurements were taken in triplicate to get the average reading for each sample. The betacyanins concentration was calculated according to Eq. (2) [25].

$$TBC\ = \frac{A \times MW \times DF}{\varepsilon \times L} \times 100 \quad (2)$$

Where, TBC is the betacyanin concentration in milligrams per litre (mg/L); *A* is the absorption value at λmax (538 nm); DF is the dilution factor; MW is the molecular weight of betacyanin (550 g/mol); ε is the molar extinction coefficient of betacyanin (60000 L/mol × cm); L is the path length of the cuvette (1 cm).

2.4.4. Determination of total phenolic content (TPC)

TPC was quantified using an optimized spectrophotometric method adapted from [26]. The analytical procedure was conducted as follows: 50 µL of appropriately diluted samples (80 µg/mL working concentration) or gallic acid standard solutions (0.01-1.00 mg/mL calibration range) were mixed with 50 µL of 1 N Folin-Ciocalteu reagent in microcentrifuge tubes. After 2 minutes of incubation at room temperature, 900 µL of sodium chloride solution (2% w/v) was added to each reaction mixture. The solutions were subsequently vortex-mixed and allowed to develop colour for 30 minutes under ambient conditions. Absorbance measurements were performed at a wavelength of 750 nm using a microplate reader with appropriate blank corrections. The quantitative determination of phenolic compounds was achieved through a linear regression analysis of the gallic acid calibration curve, with final results expressed as milligram gallic acid equivalents per 100 grams of freeze-dried sample (mg GAE/100 g FDS).

2.4.5. Determination of total flavonoid content (TFC)

A modified approach [27] was used to calculate the TFC. 30 µL of 5% $NaNO_2$ was added to 500 µL of the previously diluted sample (80 µg/mL), and then 30 µL of 10% $AlCl_3$ was added. 200 µL of 1 M NaOH was added after 6 minutes. The mixture was then topped off with 95% ethanol to reach a final volume of 1 mL, and the absorbance at 510 nm was then measured. All values were represented as mg quercetin equivalent (QE)/100 g of FDS, and the calibration curve was produced using quercetin as a standard (0.01-1.00 mg/mL).

DOI: https://doi.org/10.17509/ijost.v10i3.88934
p- ISSN 2528-1410 e- ISSN 2527-8045

2.4.6. Determination of total sugar content (TSC)

The content of total soluble sugars TSC was estimated by following the Anthrone method [28]. Briefly, the Anthrone reagent was prepared by mixing 80 mg of Anthrone with 40 mL of concentrated sulfuric acid. To 100 µL of sample mixture, 1 mL of the freshly prepared reagent was added and incubated at 90°C for 20 minutes. The intensity of the colour formed after adding the Anthrone reagent was read at 620 nm. Eq. (3) was used to measure the percentage of total sugar present in the sample mixture. And it can be used as a rough comparison of the "relative sugar content" of different extraction systems.

$$Relative\ absorbance - corrected\ sugar\ signal\ (\%) = \left(\frac{Sample\ absorbance - Blank\ absorbance}{sample\ absorbance}\right) * 100 \quad (3)$$

2.4.7. Determination of total protein content

The protein concentration in the sample will be measured using the Bradford method, and BSA with a concentration of 0.05-1 mg/mL is employed as a standard. Bradford dye of approximately 200 µL is added to 10 µL of the sample in a 96-well microplate, and the absorbance of protein is read at 595 nm [29].

2.5. Extraction Yield (EY)

To optimize the extraction conditions of anthocyanins, optimization experiments were conducted under extraction temperatures (25 - 45°C), top volume to bottom volume ratio (0.5 -2 v/v), and solid-to-liquid ratios (1:10 -1:50 g/mL). Red dragon fruit peel powder was added to each sample to form two phases, which were then separated to determine the phase volume, anthocyanins, betacyanins, total phenols, and total soluble sugars content. The extraction efficiency is determined by the phase volume ratio (R), the distribution coefficient (K) of each substance, and the recovery rate (Y) of each substance [30].

2.5.1. Phase volume ratio (R)

The *R* was defined as a ratio of the top phase volume (VT, mL) and the lower one (VB, mL) and calculated by Eq. (4).

$$R = \frac{V_T}{V_B} \quad (4)$$

2.5.2. Partition coefficient (K)

The K value was calculated by Eq. (5).

$$K = \frac{C_T}{C_B} \quad (5)$$

Where, C_T, C_B (mg/L) were the contents of compounds in the top and the lower phases, respectively, at an equilibrium state.

2.5.3. Recovery yield (Y)

The recovery yield in the top phase (Y, %) was calculated by Eq. (6).

$$Y = \frac{C_T \times V_T}{C_T \times V_T + C_B \times V_B} \times 100 \quad (6)$$

Where, C_T is the concentration (mg/L) of compounds in the top phase, and C_B is the concentration (mg/L) of compounds in the top and bottom phases. V_T and V_B denote the volumes (mL) of the top and bottom phases formed liquid biphasic system, respectively.

DOI: https://doi.org/10.17509/ijost.v10i3.88934
p- ISSN 2528-1410 e- ISSN 2527-8045

2.6. Response Surface Methodology (RSM) Design

2.6.1. Model design

In the present study, a three-factor, three-level Box-Behnken design (BBD) was employed to investigate the individual and interactive effects of process variables on the extraction process. Temperature, top volume to bottom volume ratio, and solid-liquid ratio were selected as independent variables were tabulated in **Table 2**. TAC, TBA, TPC, and TSC were selected as responses and obtained the optimum conditions for the extraction of anthocyanins from red dragon fruit peel. BBD was selected for the current research as it is effective when three variables are considered in the experimental domain with a reduced number of experiments, allowing for a more efficient and economic approach. The extraction variables with their respective levels and coded factors are also shown in **Table 2**. The complete design matrix of BBD with a total of 17 experiments is presented in **Table 3**, with experimental data for predicted and actual responses collected in the form of the extraction efficiency of TAC, TBC, TPC, and sugar. Results were fitted into the empirical second-order polynomial model, as shown in Eq. (7) [31].

$$Y = \beta_0 + \sum_{i=1}^{k} \beta_i X_i + \sum_{i=1}^{k} \beta_{ii} X_i^2 + \sum_j \sum_{i=2}^{k} \beta_{ij} X_i X_j \quad (7)$$

where Y is the response; X_i and X_j are the independent variables (i and j range from 1 to k); β_0 is the model intercept coefficient; β_j, β_{jj} and β_{ij} are interaction coefficients of linear, quadratic, and the second-order terms, respectively; k is the number of independent parameters (k = 3 in this study) [32].

Table 2. Process variables and their ranges.

Variable	Level		
	-1	**0**	**1**
Temperature (X_1, °C)	25	35	45
Solid-liquid ratio (X_2, g/mL)	2:1	1:1	2:1
Top volume to bottom volume ratio (X_3, mL/mL)	10	20	30

2.6.2. Statistical analysis

All of the analyses above were carried out in triplicate, and values are expressed as the mean. Regression analysis of the experimental data was performed using Design Expert software v. 13 (Stat-Ease, Minneapolis, Minnesota, USA). Analysis of variance (ANOVA), different statistical parameters including coefficient of determination (R^2), adjusted coefficient of determination (R_a^2) and predicted coefficient of determination (R_p^2) were all employed to check the adequacy of the developed models. Coefficient of variation (*CV*) and adequate precision were also examined to further evaluate the precision of the developed models. The significance of each term was considered when $\rho < 0.05$. In addition to the quadratic models, response surface plots were generated to establish the relationship between the independent variables and the responses.

DOI: https://doi.org/10.17509/ijost.v10i3.88934
p- ISSN 2528-1410 e- ISSN 2527-8045

Table 3. BBD experimental design and predicted resonse.[a]

Run	A (°C)	B (mg/mL)	C	TAC		TBC		TPC		TSC	
				Actual response	Predicted response	Actual response	Predicted response	Actual response	Predicted response	Actual response	Predicted response
1	35	1.25	30	0.981±0.001	0.9823	0.9524±0.001	0.9530	0.6385±0.0557	0.6534	0.5032±0.0108	0.5012
2	35	1.25	30	0.9813±0.001	0.9823	0.9582±0.0007	0.9530	0.6173±0.1646	0.6534	0.4997±0.0334	0.5012
3	45	0.5	30	0.9514±0.1142	0.9480	0.8782±0.1161	0.8709	0.8745±0.0752	0.8922	0.3373±0.0035	0.3396
4	35	1.25	30	0.9801±0.0005	0.9823	0.948±0.0008	0.9530	0.7126±0.0604	0.6534	0.5012±0.0953	0.5012
5	45	2	30	0.9807±0.0979	0.9795	0.926±0.0996	0.9290	0.9398±0.0589	0.9385	0.6576±0.0054	0.6561
6	35	2	50	0.9927±0.0865	0.9914	0.9805±0.0874	0.9748	0.9877±0.1679	0.9727	0.6562±0.0748	0.6586
7	35	0.5	10	0.9269±0.0627	0.9282	0.8248±0.0632	0.8305	0.4353±0.0489	0.4503	0.3622±0.0553	0.3582
8	25	0.5	30	0.9754±0.0146	0.9765	0.9361±0.0201	0.9331	0.3079±0.1714	0.3092	0.3497±0.1297	0.3516
9	45	1.25	50	0.9696±0.1815	0.9721	0.9209±0.1849	0.9237	0.8946±0.0161	0.9110	0.4945±0.0026	0.4923
10	25	2	30	0.99±0.0493	0.9934	0.9737±0.0429	0.9810	0.9533±0.0320	0.9356	0.6593±0.3036	0.6575
11	25	1.25	10	0.9569±0.0011	0.9544	0.8923±0.0046	0.8896	0.4484±0.1055	0.4320	0.5089±0.1709	0.5097
12	25	1.25	50	0.9898±0.1351	0.9877	0.973±0.1116	0.9714	0.6397±0.0691	0.6725	0.5012±0.199	0.4993
13	35	1.25	30	0.9803±0.0009	0.9823	0.9546±0.0015	0.9530	0.6663±0.0046	0.6534	0.4982±0.0328	0.5012
14	35	1.25	30	0.9886±0.0006	0.9823	0.952±0.0002	0.9530	0.6323±0.1959	0.6534	0.4987±0.0349	0.5012
15	35	0.5	50	0.9798±0.1383	0.9807	0.9447±0.14	0.9493	0.89±0.1675	0.8559	0.3343±0.0732	0.3330
16	35	2	10	0.9669±0.0085	0.9660	0.9156±0.0087	0.9110	0.972±0.0354	1.01	0.6552±0.0136	0.6549
17	45	1.25	10	0.9256±0.0363	0.9276	0.8215±0.0364	0.8231	0.8121±0.1225	0.7793	0.5029±0.0009	0.5034

A: Temperature; B: Solid-liquid ratio, mL/mg; C: Top volume to bottom volume ratio; TAC: Total anthocyanins content; TBC: Total Betacyanin content; TPC: Total phenolic content; TSC: Total sugar content. In order to facilitate operation, the top volume to bottom volume ratio of 1.25 should be operated as 1.2 during the experiment. [a] Values are expressed as mean ± standard deviation (n = 3).

DOI: https://doi.org/10.17509/ijost.v10i3.88934
p- ISSN 2528-1410 e- ISSN 2527-8045

2.6.3. Optimization and validation of RSM extraction models

A numerical optimization technique was performed to determine the optimum conditions for maximum TAC, TBC, TPC, and sugar. The prime conditions were identified with the desirability value of 1 for each respective response. Validation of the developed models was done by performing triplicate experiments under the optimized parameters. Finally, the average experimental results and 95% prediction interval range of predicted values were compared. This is essential to evaluate the accuracy and precision of the optimized conditions.

2.7. FTIR

The application of Fourier Transform Infrared Spectroscopy (FT-IR) spectroscopy is the study of functional groups or chemical bonds of molecules in interacting systems. FT-IR was performed using an FTIR spectrometer (Spectrum 100, Perkin Elmer, USA) at atmospheric pressure and room temperature [27]. Approximately 2 mg of samples were placed in the sample holder, the corresponding interference was scanned and recorded as a transform for the wavelength from 400 to 4000 cm^{-1} with 32 scans at a resolution of 4 cm^{-1}. Spectragryph software (version v1.2.15, Spectragryph, Germany) was used to analyse the final spectrum.

3. RESULTS AND DISCUSSION

3.1. DES-ATPS Pre-Screening

Table 4 presents a multidimensional characterization of key indicators in the anthocyanin extraction process using four types of choline-based deep eutectic solvents (DES-ATPS) aqueous two-phase systems (ChCl-1,2 BDO, ChCl-1,3 BDO, ChCl-1,4 BDO, and ChCl-urea). These indicators include antioxidant capacity (i.e., DPPH and ABTS), TAB, TBC, TFC, TPC, TSC, and protein.

Based on **Table 4**, the DPPH inhibitory activity of the top phase (T) of the ChCl-Urea system is the highest (65.53 ppm), which is significantly higher than that of other butaneglycol systems (58.51 ppm ~ 59.49 ppm). This may be related to urea acting as a strong hydrogen bond donor (HBD), enhancing the solubility of phenolic substances, which are the main antioxidant components. The ABTS activity of the ChCl-Urea system (107.62 ppm) far exceeds that of other systems (T: 71.07 ppm ~ 92.74 ppm), indicating a stronger free radical scavenging ability. In addition to that, ABTS activity is positively correlated with total phenolic content (TPC). The trend of the current finding was in agreement with a previous study done by [33], and the high TPC (405.37 mg/g) of the urea system supports this result.

The TPC and TFC of the ChCl-Urea system are 405.37 and 84.36, respectively, which are significantly higher than the maximum value of 380.39 and 68.93 in the butylene glycol system, indicating that urea is more effective in extracting phenolic substances through strong hydrogen bonding. Urea (HBD) forms a strong hydrogen bond network with ChCl (HBA), enhancing the solubility of polar substances (such as phenols and flavonoids). In contrast, the hydroxyl position of butanediol affects the spatial distribution of hydrogen bonds (for example, the linear structure of 1,4 BDO may reduce hydrogen bond density) [34]. 1,3 BDO has a higher TPC (T: 380.39 mg/g), which may be related to the optimization of the hydroxyl position that balances the distribution of phenolic substances. For TSC and Protein, the content (53.66% and 0.015 mg/mL) of the top phase in the urea system is slightly lower than that in all ethylene glycol systems (The minimum values are 54.59% and 0.51 mg/mL, respectively), while the content of the bottom phase is slightly higher. This indicates that this

DOI: https://doi.org/10.17509/ijost.v10i3.88934
p- ISSN 2528-1410 e- ISSN 2527-8045

system can efficiently extract the active components of the top phase while selectively retaining impurities such as sugar and protein in the bottom phase, which meets the core requirements of composite separation and purification. In the DES-ATPS system, the target active components (TAC, TPC, TFC, and so on) are all enriched in the top phase, and the urea-based system has a comprehensive advantage in the relevant key indicators in the top phase.

Based on the above table data and mechanism analysis, urea, as a strong hydrogen bond donor (HBD), forms a highly polar hydrogen bond network with ChCl, which better promotes the dissolution of antioxidants such as phenols and flavonoids. Therefore, in the upcoming research, we have chosen the DES-ATPS (Urea) system as the extraction solution.

Table 4. systematic evaluation of key performance indicators for Various DES-ATPS systems during the anthocyanin extraction process.

Parameters	Calibration (R^2)	DES-ATPS (Urea)		DES-ATPS (1,2 BDO)		DES-ATPS (1,3 BDO)		DES-ATPS (1,4 BDO)	
		T[a]	B[a]	T	B	T	B	T	B
DPPH (ppm)	0.9944	65.53	45.54	54.04	8.78	58.51	40.61	59.49	41.61
ABTS (ppm)	0.9945	107.62	63.69	71.07	24.76	91.31	27.5	92.74	47.98
TAC (mg/100 g)	/[b]	3.06	0.17	2.79	0.14	2.93	0.15	1.58	0.13
TBC (mg/100 g)	/[b]	1.70	0.09	1.48	0.059	1.56	0.071	1.21	0.042
TPC (mg/mL)	0.9949	405.37	149.98	331.12	144.64	380.39	144.04	364.95	152.44
TFC (mg/mL)	0.9969	84.36	5.05	60.90	22.26	68.93	5.82	57.91	5.822
TSC (%)	/[b]	53.66	46.34	64.62	35.38	56,12	43.88	54.59	45.41
Protein (mg/mL)	0.9938	0.015	0.83	0.062	0.65	0.043	0.90	0.031	0.51

[a] T: Top phase, B: Bottom phase; [b] Since TAC, TAB, and TSC were calculated directly using established formulas, no calibration curves were involved, and thus R^2 values are not applicable.

3.2. Optimization of the DES-ATPS Extraction System

The extraction conditions were mainly optimized in this section. During the extraction process, it was observed that the anthocyanins in dragon fruit peel were almost completely and selectively transferred from the mixed phase to the top phase without external force. Therefore, the following study primarily focuses on the top phase of each extraction system.

3.2.1. Influence of Extraction Parameters on Total Anthocyanin Content (TAC)

To effectively extract the target compound, it is crucial to analyse the impact of extraction parameters. This study employed a three-factor three-level BBD method to investigate the effects of various independent extraction variables on the total anthocyanin content in dragon fruit peel. Regression analysis of all three responses is presented in **Table 5**. From **Table 5**, it can be seen that the first-order terms solid-liquid ratio and top volume to bottom volume ratio have a highly significant positive impact on Y_{TAC}, while the extraction temperature has a highly significant negative impact on the reaction, indicating that the influence of specific factors on the response value is not a simple first-order linear relationship. The interaction term BC has a minor effect on the total anthocyanin content, while AC and AB have an insignificant effect on the total anthocyanin content. The quadratic term A^2 has a minor impact, while B^2 has a more significant effect. The order of factors

DOI: https://doi.org/10.17509/ijost.v10i3.88934
p- ISSN 2528-1410 e- ISSN 2527-8045

affecting the total anthocyanin content is as follows: solid-liquid ratio > top volume to bottom volume ratio > temperature. Therefore, the insignificant options were excluded from the final model in Eq. (8).

$$Y_1 = 0.9823 - 0.0106\,A + 0.0195\,B + 0.0121\,C + 0.003675\,AC - 0.0068\,BC - 0.0070\,A^2 - 0.0148\,B^2 \quad (8)$$

Figure 3 shows the response plots of TAC extraction yield generated by varying two variables at a time; this is crucial to illustrate the effects of the independent variables on extraction yield. The plots are in good agreement with regression analysis, TAC increased strongly with the solid-liquid ratio (B) and the top-to-bottom volume ratio (C), but decreased sharply as temperature (A) rose. The significant quadratic term B^2 confirms a peak-type curve with an optimal B value, peaking around a ratio of 1:48 g/mL. Beyond this point, the quadratic term (B^2) caused a decline in yield, forming a saddle-shaped surface.

Raising the temperature helps molecules move faster, which speeds up diffusion and improves the efficiency of extraction. However, anthocyanins have several phenolic hydroxyl groups (-OH), which can break down when the temperature is too high, through hydrolysis or ring-opening reactions [35, 36]. A higher solid–liquid ratio means there is more solvent available, making it easier for the solvent to interact with the plant material. But if this ratio is too high, the extraction system becomes diluted, which reduces the concentration gradient and slows down diffusion [37]. As a result, anthocyanins may not effectively transfer into the top phase [38]. In DES systems, strong hydrogen bonding helps dissolve and stabilize anthocyanins. However, when too much solvent is used, the hydrogen bond network becomes weaker, which lowers the extraction efficiency [35].

The ANOVA results (**Table 5**) show that the developed model is highly significant, with an F-value of 49.47. The determination coefficient (R^2 = 0.9845) shows that the model fits the data very well and accurately explains how the factors affect the extraction results. The adjusted R^2 (0.9646), which is very close to the original R^2, further supports this reliability. A high predicted R^2 (0.8633) suggests the model is also good at predicting new results [39]. The coefficient of variation (CV) is only 0.3951%, which is well below 10%, showing that the experimental and predicted values are very close and the method is precise and consistent [40]. Finally, the adequate precision value of 22.33 indicates a strong signal and good suitability of the model [41].

Table 5. Variance analysis for the established regression model of TAC.

Source	Sum of Squares	df	Mean Square	F-value	p-value
Model	0.0066	9	0.0007	49.47	< 0.0001
A	0.0009	1	0.0009	61.00	0.0001
B	0.0030	1	0.0030	205.39	< 0.0001
C	0.0012	1	0.0012	79.49	< 0.0001
AB	0.0000	1	0.0000	2.09	0.1915
AC	0.0001	1	0.0001	3.67	0.0971
BC	0.0002	1	0.0002	12.46	0.0096
A^2	0.0002	1	0.0002	13.97	0.0073
B^2	0.0009	1	0.0009	62.53	< 0.0001
C^2	3.354E-06	1	3.354E-06	0.2276	0.6478
Residual	0.0001	7	0.0000		
Lack of Fit	0.0001	3	0.0000	1.35	0.3766
Pure Error	0.0001	4	0.0000		
Cor Total	0.0067	16			

R^2=0.9845, R^2_{adj}=0.9646, R^2_{pred}=0.8633, Mean: 0.9716, C.V.%=0.3951, Adeq Precision: 22.3327.

DOI: https://doi.org/10.17509/ijost.v10i3.88934
p- ISSN 2528-1410 e- ISSN 2527-8045

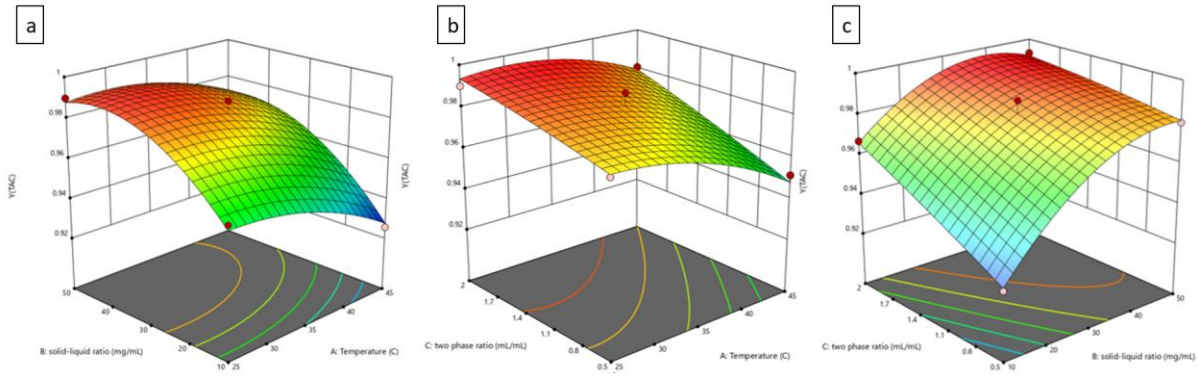

Figure 3. 3D Response surface plots demonstrating the effects of different extraction parameters on TAC: (a) solid-liquid ratio and temperature, (b) top volume to bottom volume ratio and temperature, (c) solid-liquid ratio and top volume to bottom volume ratio.

3.2.2. Influence of Extraction Parameters on Total Betacyanin Content (TBC)

All experimental results and response plots shown in **Table 6** and **Figure 4** indicate that the three extraction parameters have significant linear (A, B, C) and quadratic effects (A^2, B^2) on TBC. Further evaluation also showed that the interaction term BC had a certain influence on the response. The final developed model, excluding non-significant terms, is shown in Eq. (9).

$$Y_2 = 0.953 - 0.0286\ A + 0.0456\ B + 0.0265\ C - 0.0138\ BC - 0.0195\ A^2 - 0.0316\ B^2 \quad (9)$$

As shown in **Table 6**, the P value of this model is less than 0.0001, and the response surface regression model has reached an extremely significant level. The Lack of fit (P = 0.0579 > 0.05) is not significant, indicating that the experimental error is small. The F value of the model is 90.87, which is significant. The high value of the correlation coefficient (R^2= 0.9915) confirms the validity of the derived model, and also shows that the experimental model fits the actual experiment well. About 99.15% of the results in the actual experiment can be explained by the fitted model. The value of adjusted correlation coefficient (R^2_{adj} = 0.9806) is very close to R^2, confirming that the derived model has high significance, accuracy, and versatility. The high predicted correlation coefficient (R^2_{pred}=0.8864) further shows the adequacy of the model in predicting relationships [42]. The coefficient of variation of 0.7162% (CV < 10%) not only indicates that non-experimental factors have little effect on the results and the model has good experimental stability, but also shows that the deviation between the experimental results and the predicted results is small, with high accuracy and reliability [43]. Adequate precision of 31.0291 indicates good signal and competent model fitness [44]. Therefore, this model can be used to analyze and predict the influence of various factors on the extraction rate in anthocyanin extraction experiments.

The response surface of TBC (**Figure 4**) shows a downward trend of "slow slope". Temperature (A) and solid-liquid ratio (B) showed a slight positive effect, while the interaction term BC surface was concave, indicating that the joint action of the two was prone to negative effects. The response fluctuation range is narrower than that of TAC, indicating that the relative extraction stability of betalain is stronger.

TBC contains a pyrrole structure, and its stability is sensitive to temperature and pH. The increase in temperature helps to break the cell wall and improve the diffusion rate, but the amine and carboxyl groups in its structure are prone to thermal cracking or decarboxylation reaction, resulting in degradation [45]. The hydrogen bond environment provided by DES can temporarily stabilize betalain, but the excessive volume ratio weakens the stability of the network. The negative interaction effect of BC indicates that the greater the solvent

DOI: https://doi.org/10.17509/ijost.v10i3.88934
p- ISSN 2528-1410 e- ISSN 2527-8045

concentration, the more drastic the change in the ionic strength of the system, resulting in a decrease in the precipitation rate of betanin. This behavior may be related to the change of polarity, interfering with its charge distribution.

Table 6. Variance analysis for the established regression model of TBC.

Source	Sum of Squares	df	Mean Square	F-value	p-value
Model	0.0360	9	0.0040	90.87	< 0.0001
A	0.0065	1	0.0065	148.18	< 0.0001
B	0.0166	1	0.0166	377.90	< 0.0001
C	0.0056	1	0.0056	127.56	< 0.0001
AB	0.0001	1	0.0001	1.98	0.2017
AC	0.0000	1	0.0000	0.5906	0.4673
BC	0.0008	1	0.0008	17.17	0.0043
A^2	0.0016	1	0.0016	36.38	0.0005
B^2	0.0042	1	0.0042	95.51	< 0.0001
C^2	0.0001	1	0.0001	2.42	0.1637
Residual	0.0003	7	0.0000		
Lack of Fit	0.0003	3	0.0001	6.01	0.0579
Pure Error	0.0001	4	0.0000		
Cor Total	0.0363	16			

R^2=0.9915, R^2_{adj}=0.9806, R^2_{pred}=0.8864, Mean= 0.9266, C.V.%=0.7162, Adeq Precision: 31.0291.

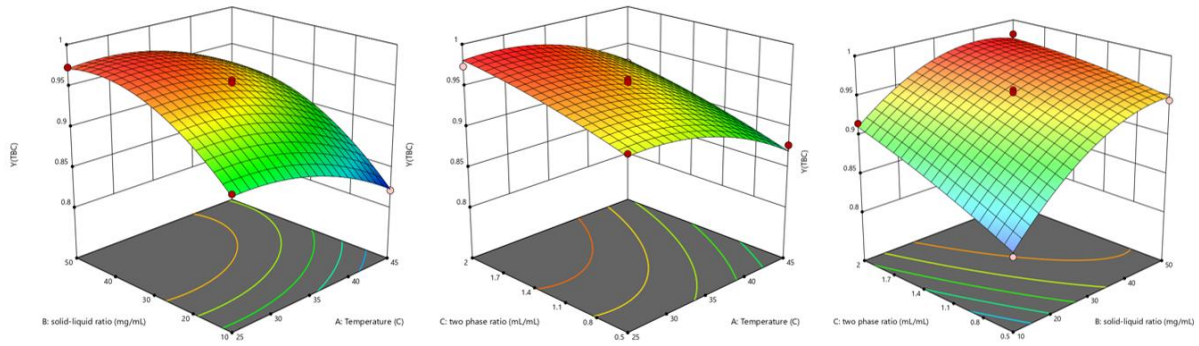

(a) (b) (c)

Figure 4. 3D Response surface plots demonstrating the effects of different extraction parameters on TBC: (a) solid-liquid ratio and temperature, (b) top volume to bottom volume ratio and temperature, (c) solid-liquid ratio and top volume to bottom volume ratio.

3.2.3. Influence of Extraction Parameters on Total Phenolic Content (TPC)

From **Table 7** and **Figure 5**, the linear terms in the regression equation indicate that temperature (A), solid-liquid ratio (B), and top volume to bottom volume ratio (C) have a very significant impact on TPC, and these two extraction parameters （B and C） have a positive effect on the quadratic terms. For the response of TPC, the interaction between temperature and the top volume to bottom volume ratio shows a moderately significant negative impact. The remaining two terms (including the remaining two) are not significant. Therefore, they were excluded from the final developed model, as shown in Eq. (10).

$Y_3 = 0.6534 + 0.1465\ A + 0.09303\ B + 0.1681\ C - 0.1450\ AC - 0.1098\ BC + 0.04884\ B^2 + 0.0195\ C^2$ (10)

Based on the statistical analysis, the developed model was found to be significant at an F-value of 44.72. High values of R^2 (0.9829) and R^2_{adj} (0.9609) indicates a high degree of

DOI: https://doi.org/10.17509/ijost.v10i3.88934
p- ISSN 2528-1410 e- ISSN 2527-8045

correlation. The predicted correlation coefficient (R^2_{pred} = 0.8451) was also determined to be of high significance. In addition, values of coefficient of variation (C.V.% = 5.6) and adequate precision (Adeq Precision = 22.1893) further indicate the ability of the deduced model to define the relation between the extraction variables and the response of TPC.

Table 7. Variance analysis for the established regression model of TPC.

Source	Sum of Squares	df	Mean Square	F-value	p-value
Model	0.6749	9	0.0750	44.72	< 0.0001
A	0.1716	1	0.1716	102.35	< 0.0001
B	0.0692	1	0.0692	41.29	0.0004
C	0.2262	1	0.2262	134.88	< 0.0001
AB	0.0030	1	0.0030	1.76	0.2257
AC	0.0841	1	0.0841	50.18	0.0002
BC	0.0482	1	0.0482	28.74	0.0011
A²	0.0001	1	0.0001	0.0314	0.8643
B²	0.0100	1	0.0100	5.99	0.0443
C²	0.0596	1	0.0596	35.57	0.0006
Residual	0.0117	7	0.0017		
Lack of Fit	0.0061	3	0.0020	1.44	0.3559
Pure Error	0.0056	4	0.0014		
Cor Total	0.6866	16			

R^2=0.9829, R^2_{adj}=0.9609, R^2_{pred}=0.8451, Mean= 0.7307, C.V.%=5.6, Adeq Precision: 22.1893.

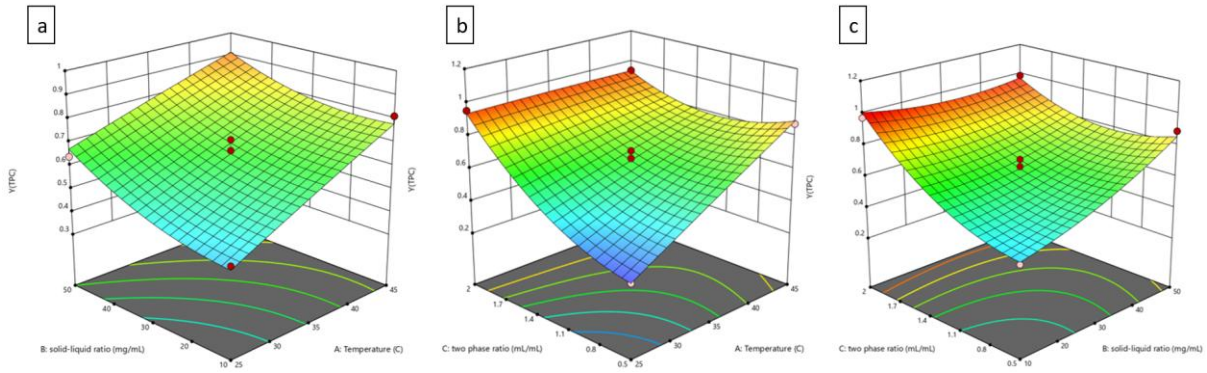

Figure 5. 3D Response surface plots demonstrating the effects of different extraction parameters on TPC: (a) solid-liquid ratio and temperature, (b) top volume to bottom volume ratio and temperature, (c) solid-liquid ratio and top volume to bottom volume ratio.

3.2.4. Influence of Extraction Parameters on Total Sugar Content (TSC)

The regression model for TSC displayed the highest statistical performance among all four models, with an R^2 of 0.9995, adjusted R^2 of 0.9989, and predicted R^2 of 0.9937 (**Table 8** as well as **Figures 6 and 7**). These values reflect a near-perfect correlation between the model and the experimental data. The C.V.% was 0.7118, and the Adequate Precision reached 118.3619 exceptionally high value that reflects outstanding model precision and signal strength.

All three main effects (A, B, and C) were extremely significant ($p < 0.0001$), with factor C contributing the most dramatically (F = 14674.54), suggesting that this parameter overwhelmingly governs sugar extraction efficiency. In contrast to other models, all quadratic terms (e.g., A^2, B^2, C^2) and interaction (AB) were not statistically significant ($p > 0.05$), indicating a predominantly linear relationship in the TSC model. This suggests that sugar

DOI: https://doi.org/10.17509/ijost.v10i3.88934
p- ISSN 2528-1410 e- ISSN 2527-8045

partitioning into the top phase is more straightforward and less influenced by nonlinear or interactive effects.

Monosaccharides and disaccharides are thermally stable and not prone to degradation. Their extraction is governed primarily by solvent–solute diffusion across the phase interface. Temperature increases reduce solution viscosity, improving diffusion but not altering sugar structure [46]. Hence, the extraction behaves linearly with extraction conditions. The final developed model, excluding the insignificant terms, is shown in Eq. (11).

$$Y_4 = 0.5002 - 0.005813\ A - 0.005375\ B + 0.1531\ C + 0.0076\ AC + 0.007225\ BC \quad (11)$$

Table 8. Variance analysis for the established regression model of TSC.

Source	Sum of Squares	df	Mean Square	F-value	p-value
Model	0.1886	9	0.0210	1639.34	< 0.0001
A	0.0003	1	0.0003	21.14	0.0025
B	0.0002	1	0.0002	18.08	0.0038
C	0.1876	1	0.1876	14674.54	< 0.0001
AB	1.225E-07	1	1.225E-07	0.0096	0.9248
AC	0.0002	1	0.0002	18.07	0.0038
BC	0.0002	1	0.0002	16.33	0.0049
A^2	0.0000	1	0.0000	2.58	0.1521
B^2	5.329E-06	1	5.329E-06	0.4168	0.5391
C^2	0.0000	1	0.0000	2.77	0.1400
Residual	0.0001	7	0.0000		
Lack of Fit	0.0001	3	0.0000	5.90	0.0597
Pure Error	0.0000	4	4.125E-06		
Cor Total	0.1887	16			

R^2=0.9995, R^2_{adj}=0.9989, R^2_{pred}=0.9937, Mean: 0.5024, C.V.%=0.7118, Adeq Precision: 118.3619.

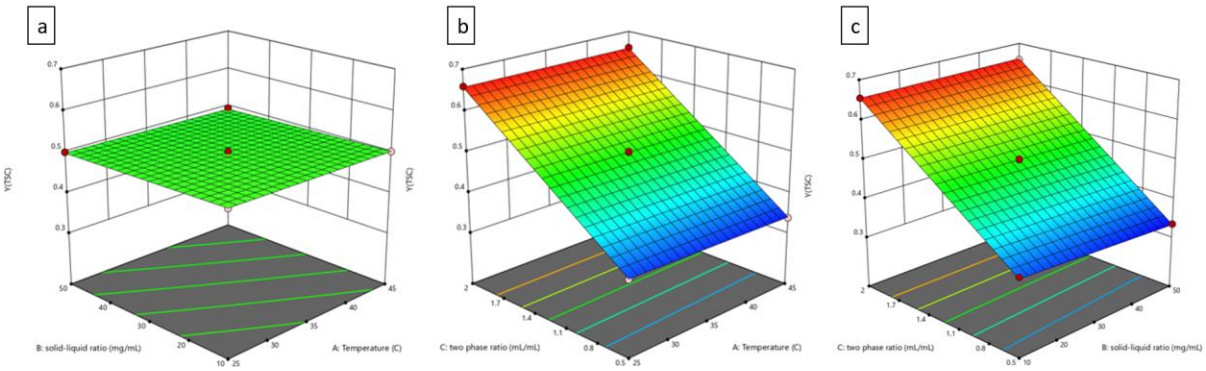

Figure 6. 3D Response surface plots demonstrating the effects of different extraction parameters on TSC: (a) solid-liquid ratio and temperature, (b) top volume to bottom volume ratio and temperature, (c) solid-liquid ratio and top volume to bottom volume ratio.

In summary, the extraction behavior of different products shows different response mechanisms. The responses of TAC and TPC to temperature, solid-liquid ratio and phase volume ratio are more complex, involving the dual effects of degradation and oxidation; TBC is more sensitive to the change of volume ratio, indicating that its solubility is closely related to charge stability; and TSC is a typical diffusion-controlled behavior, with stable structure and linear response. The 3D response surface provides an intuitive basis for the optimization of extraction conditions and reveals the migration and stabilization mechanism at the molecular level.

DOI: https://doi.org/10.17509/ijost.v10i3.88934
p- ISSN 2528-1410 e- ISSN 2527-8045

The regression models established for TAC, TBC, TPC, and TSC all demonstrated high significance ($p < 0.0001$) and strong fitting performance ($R^2 > 0.98$). The relatively close values of adjusted and predicted R^2, along with high Adequate Precision and low coefficients of variation (C.V.%), confirmed the models' robustness and reliability.

Notably, the extraction of TAC and TBC was affected not only by individual factors but also by their interactions and quadratic effects, indicating complex synergistic mechanisms. In contrast, the TSC model showed a dominant linear contribution from factor C, suggesting a more stable and straightforward extraction behavior. These findings provide a solid statistical and mechanistic foundation for optimizing DES-ATPS conditions for the efficient extraction of various bioactive components.

All four regression models (TAC, TBC, TPC, and TSC) showed high levels of accuracy and predictive power, with R^2 values exceeding 0.98. The models for TAC, TBC, and TPC revealed that both linear and nonlinear effects, as well as factor interactions, play a crucial role in the extraction of anthocyanins, betacyanins, and phenolics. This highlights the complex nature of polyphenol and pigment partitioning behavior in DES-ATPS systems. In contrast, the TSC model was dominated by a single linear effect (factor C), implying that sugar extraction is less sensitive to interactive or nonlinear influences.

These results not only confirm the reliability of the established models but also provide mechanistic insight into how different components respond to extraction variables. This lays a solid foundation for future optimization of the DES-ATPS system to achieve efficient and selective extraction of bioactive compounds.

3.3. RSM Optimization and Model Verification

Through the analysis of the regression equation using Design-Expert software, the optimal extraction conditions were obtained: the solid-liquid ratio is 47.499, the temperature is 32.541, and the top volume to bottom volume ratio is 1.741; the theoretical yield of anthocyanin extraction is 0.993. To verify the reliability of this method, considering the experimental conditions and the feasibility of actual operation, the optimal process parameters were adjusted to a solid-liquid ratio of 48, a temperature of 33, and a top volume to bottom volume ratio of 1.7. Under these conditions, verification experiments for anthocyanin extraction were conducted and repeated three times, with an average anthocyanin extraction rate of 0.995. The difference from the previous experiment was 0.002. This indicates that the model can effectively simulate and predict the extraction yield of anthocyanins from red dragon fruit peel, thereby demonstrating the feasibility of using RSM to optimize the extraction conditions for anthocyanins.

3.4. Fourier Transform Infrared Spectroscopic Characterization of Anthocyanin Extraction Products

FTIR analysis (**Figure 7**) confirms that the ChCl: Urea DES maintained excellent structural stability throughout the extraction process, while anthocyanins were successfully transferred into the top phase. Detailed information regarding how to read FTIR is explained elsewhere [47-51]. As shown in the spectra, both pre- and post-extraction DES samples (blue and red curves) exhibit a broad O-H/N-H stretching vibration band around 3300 cm^{-1}, attributed to extensive hydrogen bonding between choline and urea, indicating the DES structure remained intact. The characteristic peaks for C-H stretching (~2900 cm^{-1}), C=O stretching from urea (~1650 cm^{-1}), and N-H bending (~1550 cm^{-1}) were consistently observed before and after extraction, further confirming the chemical integrity and potential recyclability of the DES

DOI: https://doi.org/10.17509/ijost.v10i3.88934
p- ISSN 2528-1410 e- ISSN 2527-8045

system, which would make it a promising alternative to existing extraction methods in large-scale industrial production.

Moreover, the post-extraction top phase (red curve) showed significantly enhanced peaks near 1650 and 1550 cm^{-1}, corresponding to the aromatic C=C vibrations of anthocyanin molecules, indicating successful extraction from dragon fruit peel. Additionally, increased intensity at ~3300 cm^{-1} suggests the introduction of polyphenolic -OH groups from anthocyanins. Importantly, no major peak shifts or losses were observed, and no degradation-associated bands emerged, implying that the structure of anthocyanins was preserved and the DES remained chemically stable and reusable [52].

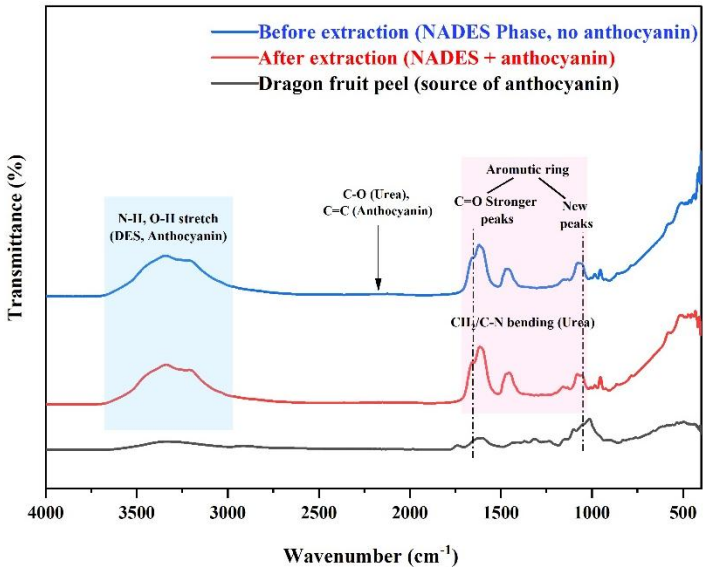

Figure 7. Fourier transform infrared spectroscopy of the two-phase solutions before and after ChCl-urea extraction, as well as the top phase solution of the extraction. The blue line represents the top phase of the DES before adding dragon fruit peel powder, and the red line represents the top phase of the extract solution rich in DES. The black line represents the dragon fruit peel powder.

3.5. Contribution to Sustainable Development Goals (SDGs)

The optimized extraction of anthocyanins from red dragon fruit peel using a choline chloride–urea DES-ATPS system demonstrates a strong alignment with several key SDGs.

(i) This work directly contributes to SDG 3: Good Health and Well-being by facilitating the production of natural antioxidants with known health-promoting properties, such as anti-inflammatory, anti-carcinogenic, and cardioprotective effects. Anthocyanins, when extracted in high yield and purity without degradation, can be utilized in functional foods, nutraceuticals, and natural supplements, offering a safer alternative to synthetic additives.

(ii) The study advances SDG 9: Industry, Innovation and Infrastructure by introducing a scalable, low-energy, and solvent-efficient extraction method. The use of DES represents a shift away from conventional hazardous organic solvents and energy-intensive techniques, providing a green innovation in the food and pharmaceutical industries. Furthermore, the demonstrated robustness of the statistical models (R^2 > 0.98) offers a reproducible framework for industrial-scale process optimization.

(iii) This method supports SDG 12: Responsible Consumption and Production by valorizing agricultural waste, specifically the peels of red dragon fruit, which are typically

DOI: https://doi.org/10.17509/ijost.v10i3.88934
p- ISSN 2528-1410 e- ISSN 2527-8045

discarded. By converting biomass into valuable bioactive compounds, the process embodies the principles of a circular economy and sustainable bioprocessing. The reuse potential of DES and the reduction in energy consumption further enhance the environmental sustainability of the method.

Collectively, these outcomes show that the developed DES-ATPS extraction process not only achieves high technical efficiency but also contributes meaningfully to the global agenda for sustainable development. The integration of green chemistry principles with applied food science provides a blueprint for responsible innovation and resource-efficient production. Finally, this study adds new information regarding SDGs as reported elsewhere (**Table 9**).

Table 9. Previous studies on SDGs.

No	Title	Reference
1	Effect of substrate and water on cultivation of Sumba seaworm (nyale) and experimental practicum design for improving critical and creative thinking skills of prospective science teacher in biology and supporting sustainable development goals (SDGs).	[53]
2	Characteristics of jengkol peel (Pithecellobium jiringa) biochar produced at various pyrolysis temperatures for enhanced agricultural waste management and supporting sustainable development goals (SDGs).	[54]
3	Contributing factors to greenhouse gas emissions in agriculture for supporting sustainable development goals (SDGs): Insights from a systematic literature review completed by computational bibliometric analysis.	[55]
4	Integrated CRITIC-TOPSIS and Monte Carlo sensitivity analysis for optimal various natural fibre selection in sustainable building insulation composites to support the Sustainable Development Goals (SDGs).	[56]
5	Current strategies for mitigating airborne pathogen transmission: An integrative review based on aerosol science and particle technology to support the Sustainable Development Goals (SDGs), complemented by a bibliometric analysis.	[57]
6	Development of interpolymer complexes for soil structure and water retention: A scientific and technological contribution to Sustainable Development Goals (SDGs).	[58]
7	What evidence supports the advancement of language learning through digital innovation? Toward achieving Sustainable Development Goals (SDGs) in the 21st century completed with bibliometric analysis.	[59]
8	Developing an inclusive ICT-based academic information system using REST API to promote Sustainable Development Goals (SDGs) in higher education.	[60]
9	Sustainable packaging: Bioplastics as a low-carbon future step for the sustainable development goals (SDGs).	[61]
10	Production of wet organic waste ecoenzymes as an alternative solution for environmental conservation supporting sustainable development goals (SDGs): A techno-economic and bibliometric analysis.	[62]
11	Hazard identification, risk assessment, and determining control (HIRADC) for workplace safety in manufacturing industry: A risk-control framework complete with bibliometric literature review analysis to support sustainable development goals (SDGs).	[63]
12	Techno-economic analysis of production ecobrick from plastic waste to support sustainable development goals (SDGs).	[64]
13	Techno-economic analysis of sawdust-based trash cans and their contribution to Indonesia's green tourism policy and the sustainable development goals (SDGs).	[65]
14	Physical adaptation of college students in high-altitude training: Empirical findings and curriculum development insights to support Sustainable Development Goals (SDGs).	[66]

DOI: https://doi.org/10.17509/ijost.v10i3.88934
p- ISSN 2528-1410 e- ISSN 2527-8045

Table 9 (continue). Previous studies on SDGs.

No	Title	Reference
15	Enhancing job satisfaction through human resource information systems and communication: A commitment-based approach to achieve Sustainable Development Goals (SDGs) in education-oriented organizations.	[67]
16	Sustainable development goals (SDGs) in science education: Definition, literature review, and bibliometric analysis.	[68]
17	Experimental demonstration for teaching the concept of steam engine power plant to vocational students to support the Sustainability Development Goals (SDGs) and its comparison to Indonesian Merdeka Curriculum.	[69]
18	Internet of things-based child stunting detection system for supporting sustainable development goals.	[70]
19	AppSheets on wetlands to realize sustainable development goals (SDGs).	[71]
20	Utilization of orange peel-derived biochar for ammonia adsorption: Isotherm analysis and hydrogen storage prospective for supporting sustainable development goals (SDGs).	[72]
21	Global warming: Promoting environmental awareness of senior secondary school students facing issues in the Sustainable Development Goals (SDGs).	[73]
22	Fabrication of resin-based brake pad from snake fruit peel as sustainable renewable resources to support sustainable development goals (SDGs).	[74]
23	Adsorption isotherm characteristics of calcium carbon microparticles prepared from chicken bone waste to support sustainable development goals (SDGs).	[75]
24	Computational calculation of adsorption isotherm characteristics of carbon microparticles prepared from mango seed waste to support sustainable development goals (SDGs).	[76]
25	Bibliometric analysis of the use of biochar in an environmental law perspective.	[77]
26	Project effectivity of adsorbent from food waste for handling wastewater as a learning strategy to learning achievement of education for sustainable development and inquiry abilities.	[78]
27	Production of pen holders from can waste for supporting sustainable development goals (SDGs): Technology and cost analysis.	[79]
28	Gender equality education through augmented reality (AR)-based flashcards in learning social studies education in schools as an embodiment of sustainable development goals (SDGs).	[80]
29	Profile (Knowledge, Attitude, and Practice) of sustainable science teacher at junior high schools in Riau towards the Sustainable Development Goals (SDGs).	[81]
30	Red onion peel biomass carbon microparticles for ammonia adsorption for supporting hydrogen storage and sustainable development goals (SDGs) with isotherm analysis.	[82]

4. CONCLUSION

This study has successfully utilized green organic solvent DES (ChCl: Urea 1:2)-ATPS to extract anthocyanins from the peel of red dragon fruit. Based on single factor Box-Behnken central composite design method, our study suggested that the optimum solid-liquid ratio is 47.50, the temperature is 32.50, and the top volume to bottom volume ratio is 1.741. Under these conditions, the anthocyanin extraction rate obtained is close to the predicted value optimized by the response surface method, indicating the feasibility of the optimization plan. The results of this study provide technical support for the industrial production of anthocyanins extracted from red dragon fruit peels, offer theoretical basis and optimized process parameters for the deep utilization of red dragon fruit peels, and have certain guiding significance for the comprehensive utilization of red dragon fruit peels. Characterization

DOI: https://doi.org/10.17509/ijost.v10i3.88934
p- ISSN 2528-1410 e- ISSN 2527-8045

results indicate that both anthocyanins and the DES solution are well protected in the DES-K_2HPO_4 composite top phase, which facilitates efficient extraction of anthocyanins. The physicochemical properties of the DES remain unchanged, supporting its potential for sustainable reuse. The extraction method proposed in this study, along with the employed extractant, demonstrates promising scalability and environmental compatibility for anthocyanin extraction. Using red dragon fruit peel as a raw material offers a safer and more sustainable solution for future large-scale anthocyanin production.

5. ACKNOWLEDGMENT

The authors would like to acknowledge Xiamen University Malaysia, for providing financial support under the Xiamen University Malaysia Research Fund, XMUMRF/2024-C14/IENG/0076.

6. AUTHORS' NOTE

The authors declare that there is no conflict of interest regarding the publication of this article. The authors confirmed that the paper was free of plagiarism.

7. REFERENCES

[1] Jiang, X., Lu, Y., and Liu, S. Q. (2020). Effects of pectinase treatment on the physicochemical and oenological properties of red dragon fruit wine fermented with Torulaspora delbrueckii. *Lwt*, *132*, 109929.

[2] Nandiyanto, A. B. D., Maryanti, R., Fiandini, M., Ragadhita, R., Usdiyana, D., Anggraeni, S., and Al-Obaidi, A. S. M. (2020). Synthesis of carbon microparticles from red dragon fruit (Hylocereus undatus) peel waste and their adsorption isotherm characteristics. *Molekul*, *15*(3), 199-209.

[3] Jiang, H., Zhang, W., Li, X., Shu, C., Jiang, W., and Cao, J. (2021). Nutrition, phytochemical profile, bioactivities and applications in food industry of pitaya (Hylocereus spp.) peels: A comprehensive review. *Trends in Food Science & Technology*, *116*, 199-217.

[4] Ramadhan, M. O., and Handayani, M. N. (2021). Anthocyanins from agro-waste as time-temperature indicator to monitor freshness of fish products. *ASEAN Journal of Science and Engineering*, *1*(2), 67-72.

[5] Wallace, T. C., and Giusti, M. M. (2019). Anthocyanins—nature's bold, beautiful, and health-promoting colors. *Foods*, *8*(11), 550.

[6] Huang, Y. L., Yin, J. R., Zhao, X., Luo, Y. D., Zhang, Z. F., Zhao, P. R., and Chen, X. L. (2022). Fermentation process optimization and antioxidant activity analysis of Docynia delavayi (Franch.) Schneid. and red dragon fruit compound wine. *Journal of Food Safety and Quality*, *13*(8), 2672-2679.

[7] Raj, G. B., and Dash, K. K. (2020). Ultrasound-assisted extraction of phytocompounds from dragon fruit peel: Optimization, kinetics and thermodynamic studies. *Ultrasonics Sonochemistry*, *68*, 105180.

[8] Thuy, N. M., Ngoc, P. T. B., and Tai, N. V. (2022). Effect of conventional and ultrasonic-assisted extracts on betacyanin content of red dragon fruit (Hylocereus polyrhizus). *Food Research*, *6*(3), 389-395.

[9] Thirugnanasambandham, K., and Sivakumar, V. (2017). Microwave assisted extraction process of betalain from dragon fruit and its antioxidant activities. *Journal of the Saudi Society of Agricultural Sciences*, *16*(1), 41-48.

[10] Van, M. P., Duc, D. T., Thanh, H. D. T., and Chi, H. T. (2020). Comparison of ultrasound assisted extraction and enzyme assisted extraction of betacyanin from red dragon fruit peel. In *E3S Web of Conferences*, *187*, 04004.
[11] Huang, C., Xu, W., Mo, Z., Lu, Q., and Huang, Y. (2023). Optimization of anthocyanin extraction process and analysis of anthocyanin composition in pericarp of red pitaya. *Food Science and Technology*, *48*(09), 183-191.
[12] Zannou, O., Pashazadeh, H., Ghellam, M., Ibrahim, S. A., and Koca, I. (2021). Extraction of anthocyanins from borage (Echium amoenum) flowers using choline chloride and a glycerol-based, deep eutectic solvent: Optimization, antioxidant activity, and in vitro bioavailability. *Molecules*, *27*(1), 134.
[13] Velásquez, P., Bustos, D., Montenegro, G., and Giordano, A. (2021). Ultrasound-assisted extraction of anthocyanins using natural deep eutectic solvents and their incorporation in edible films. *Molecules*, *26*(4), 984.
[14] Radošević, K., Ćurko, N., Srček, V. G., Bubalo, M. C., Tomašević, M., Ganić, K. K., and Redovniković, I. R. (2016). Natural deep eutectic solvents as beneficial extractants for enhancement of plant extracts bioactivity. *Lwt*, *73*, 45-51.
[15] Fuad, F. M., Nadzir, M. M., and Harun, A. (2021). Hydrophilic natural deep eutectic solvent: A review on physicochemical properties and extractability of bioactive compounds. *Journal of Molecular Liquids*, *339*, 116923.
[16] Bentley, J., Olsen, E. K., Moore, J. P., and Farrant, J. M. (2020). The phenolic profile extracted from the desiccation-tolerant medicinal shrub Myrothamnus flabellifolia using Natural Deep Eutectic Solvents varies according to the solvation conditions. *Phytochemistry*, *173*, 112323.
[17] Benvenutti, L., Zielinski, A. A. F., and Ferreira, S. R. S. (2019). Which is the best food emerging solvent: IL, DES or NADES?. *Trends in Food Science & Technology*, *90*, 133-146.
[18] García, A., Rodríguez-Juan, E., Rodríguez-Gutiérrez, G., Rios, J. J., and Fernández-Bolaños, J. (2016). Extraction of phenolic compounds from virgin olive oil by deep eutectic solvents (DESs). *Food Chemistry*, *197*, 554-561.
[19] Buarque, F. S., Gautério, G. V., Coelho, M. A. Z., Lemes, A. C., and Ribeiro, B. D. (2022). Aqueous two-phase systems based on ionic liquids and deep eutectic solvents as a tool for the recovery of non-protein bioactive compounds—a review. *Processes*, *11*(1), 31.
[20] Wang, T., Xu, W. J., Wang, S. X., Kou, P., Wang, P., Wang, X. Q., and Fu, Y. J. (2017). Integrated and sustainable separation of chlorogenic acid from blueberry leaves by deep eutectic solvents coupled with aqueous two-phase system. *Food and Bioproducts Processing*, *105*, 205-214.
[21] Tee, L. H., Yang, B., Tey, B. T., Chan, E. S., Azlan, A., Ismail, A., and Prasad, K. N. (2017). Valorization of Dacryodes rostrata fruit through the characterization of its oil. *Food Chemistry*, *235*, 257-264.
[22] Bhatnagar, A. S., and Krishna, A. G. (2013). Natural antioxidants of the Jaffna variety of Moringa Oleifera seed oil of Indian origin as compared to other vegetable oils. *Grasas y Aceites*, *64*(5), 537-545.
[23] Thavamoney, N., Sivanadian, L., Tee, L. H., Khoo, H. E., Prasad, K. N., and Kong, K. W. (2018). Extraction and recovery of phytochemical components and antioxidative properties in fruit parts of Dacryodes rostrata influenced by different solvents. *Journal of Food Science and Technology*, *55*(7), 2523-2532.
[24] Zitha, E. Z. M., Magalhães, D. S., do Lago, R. C., Carvalho, E. E. N., Pasqual, M., and Boas, E. V. D. B. V. (2022). Changes in the bioactive compounds and antioxidant activity in red-fleshed dragon fruit during its development. *Scientia Horticulturae*, *291*, 110611.

DOI: https://doi.org/10.17509/ijost.v10i3.88934
p- ISSN 2528-1410 e- ISSN 2527-8045

[25] Lim, T. W., Lim, R. L. H., Pui, L. P., Tan, C. P., and Ho, C. W. (2023). Synergistic enhancing effect of xanthan gum, carboxymethyl cellulose and citric acid on the stability of betacyanins in fermented red dragon fruit (Hylocereus polyrhizus) drink during storage. *Heliyon*, *9*(10), e21025

[26] Johnson, J. B., Mani, J. S., and Naiker, M. (2023). Microplate methods for measuring phenolic content and antioxidant capacity in chickpea: Impact of shaking. *Engineering Proceedings*, *48*(1), 57.

[27] Ayele, D. T., Akele, M. L., and Melese, A. T. (2022). Analysis of total phenolic contents, flavonoids, antioxidant and antibacterial activities of Croton macrostachyus root extracts. *BMC Chemistry*, *16*(1), 30.

[28] Qi, W., Bai, J., Yu, H., and Han, G. (2025). Physiological adaptations of vigna radiata to heavy metal stress: Soluble sugar accumulation and biomass enhancement. *Plants*, *14*(8), 1191.

[29] Moreira, D. C. (2022). RGBradford: Accurate measurement of protein concentration using a smartphone camera and the blue to green intensity ratio. *Analytical Biochemistry*, *655*, 114839.

[30] Vo, T. N., Tran, M. T., and Hoang, M. H. (2023). Extraction of betacyanins from hylocereus polyrhizus peels using aqueous two-phase system. *Journal of Technical Education Science*, *18*(Special Issue 01), 8-16.

[31] Thirugnanasambandham, K., Sivakumar, V., and Maran, J. P. (2014). Process optimization and analysis of microwave assisted extraction of pectin from dragon fruit peel. *Carbohydrate Polymers*, *112*, 622-626.

[32] Moorthy, I. G., Maran, J. P., Ilakya, S., Anitha, S. L., Sabarima, S. P., and Priya, B. (2017). Ultrasound assisted extraction of pectin from waste Artocarpus heterophyllus fruit peel. *Ultrasonics Sonochemistry*, *34*, 525-530.

[33] Da, L. I., Congyu, M. A., Qinglin, L. Y. U., Wenyuan, L. I. U., Feng, F. E. N. G., and Jie, Z. H. A. N. G. (2018). Total phenolic contents and bioactivities of defatted Vitellaria paradoxa kernels from different origin. *Journal of China Pharmaceutical University*, *49*(5), 572-579.

[34] Melavanki, R., Muddapur, G. V., Srinivasa, H. T., Honnanagoudar, S. S., and Patil, N. R. (2021). Solvation, rotational dynamics, photophysical properties study of aromatic asymmetric di-ketones: An experimental and theoretical approach. *Journal of Molecular Liquids*, *337*, 116456.

[35] He, B., Zhang, L. L., Yue, X. Y., Liang, J., Jiang, J., Gao, X. L., and Yue, P. X. (2016). Optimization of ultrasound-assisted extraction of phenolic compounds and anthocyanins from blueberry (Vaccinium ashei) wine pomace. *Food Chemistry*, *204*, 70-76.

[36] Ghitescu, R. E., Volf, I., Carausu, C., Bühlmann, A. M., Gilca, I. A., and Popa, V. I. (2015). Optimization of ultrasound-assisted extraction of polyphenols from spruce wood bark. *Ultrasonics Sonochemistry*, *22*, 535-541.

[37] Avhad, D. N., and Rathod, V. K. (2015). Ultrasound assisted production of a fibrinolytic enzyme in a bioreactor. *Ultrasonics Sonochemistry*, *22*, 257-264.

[38] Zhuang, D., Chew, K. W., Teoh, W. Y., Al-Maari, M. A. S., Hizaddin, H. F., Alharthi, S., and Ling, T. C. (2023). Extraction of phycocyanin from Spirulina using deep eutectic solvent liquid biphasic system. *Journal of the Taiwan Institute of Chemical Engineers*, *151*, 105125.

DOI: https://doi.org/10.17509/ijost.v10i3.88934
p- ISSN 2528-1410 e- ISSN 2527-8045

[39] Maran, J. P., Sivakumar, V., Sridhar, R., and Immanuel, V. P. (2013). Development of model for mechanical properties of tapioca starch based edible films. *Industrial Crops and Products*, *42*, 159-168.
[40] He, B., Zhang, L. L., Yue, X. Y., Liang, J., Jiang, J., Gao, X. L., and Yue, P. X. (2016). Optimization of ultrasound-assisted extraction of phenolic compounds and anthocyanins from blueberry (Vaccinium ashei) wine pomace. *Food Chemistry*, *204*, 70-76.
[41] Maran, J. P., Manikandan, S., Thirugnanasambandham, K., Nivetha, C. V., and Dinesh, R. (2013). Box–Behnken design based statistical modeling for ultrasound-assisted extraction of corn silk polysaccharide. *Carbohydrate Polymers*, *92*(1), 604-611.
[42] Maran, J. P., Sivakumar, V., Sridhar, R., and Immanuel, V. P. (2013). Development of model for mechanical properties of tapioca starch based edible films. *Industrial Crops and Products*, *42*, 159-168.
[43] He, B., Zhang, L. L., Yue, X. Y., Liang, J., Jiang, J., Gao, X. L., and Yue, P. X. (2016). Optimization of ultrasound-assisted extraction of phenolic compounds and anthocyanins from blueberry (Vaccinium ashei) wine pomace. *Food Chemistry*, *204*, 70-76.
[44] Maran, J. P., Manikandan, S., Thirugnanasambandham, K., Nivetha, C. V., and Dinesh, R. (2013). Box–Behnken design based statistical modeling for ultrasound-assisted extraction of corn silk polysaccharide. *Carbohydrate Polymers*, *92*(1), 604-611.
[45] Das, M., Saeid, A., Hossain, M. F., Jiang, G. H., Eun, J. B., and Ahmed, M. (2019). Influence of extraction parameters and stability of betacyanins extracted from red amaranth during storage. *Journal of Food Science and Technology*, *56*(2), 643-653.
[46] Idenaga, S., Hosoya, T., and Miyafuji, H. (2024). The possibility of chemical transformation of glucose in choline chloride/glucose deep eutectic solvent with thermal instability. *RSC Advances*, *14*(24), 17022-17031.
[47] Nandiyanto, A. B. D., Oktiani, R., and Ragadhita, R. (2019). How to read and interpret FTIR spectroscope of organic material. *Indonesian Journal of Science and Technology*, *4*(1), 97-118.
[48] Nandiyanto, A. B. D., Ragadhita, R., and Fiandini, M. (2023). Interpretation of Fourier transform infrared spectra (FTIR): A practical approach in the polymer/plastic thermal decomposition. *Indonesian Journal of Science and Technology*, *8*(1), 113-126.
[49] Sukamto, S., and Rahmat, A. (2023). Evaluation of FTIR, macro and micronutrients of compost from black soldier fly residual: In context of its use as fertilizer. *ASEAN Journal of Science and Engineering*, *3*(1), 21-30.
[50] Obinna, E. M. (2022). Physicochemical properties of human hair using Fourier transform infra-red (FTIR) and scanning electron microscope (SEM). *ASEAN Journal for Science and Engineering in Materials*, *1*(2), 71-74.
[51] Nandiyanto, A. B. D., Putri, A. R., Pratiwi, V. A., Ilhami, V. I. N., Kaniawati, I., Kurniawan, T., and Bilad, M. R. (2024). Fourier transform infrared spectroscopy (FTIR) of pyrolysis of polypropylene microparticles and its chemical reaction mechanism completed with computational bibliometric literature review to support sustainable development goals (SDGs). *Journal of Engineering, Science and Technology*, *19*(3), 1090-1104.
[52] Zhuang, D., Chew, K. W., Teoh, W. Y., Al-Maari, M. A. S., Hizaddin, H. F., Alharthi, S., and Ling, T. C. (2023). Extraction of phycocyanin from Spirulina using deep eutectic solvent liquid biphasic system. *Journal of the Taiwan Institute of Chemical Engineers*, *151*, 105125.

DOI: https://doi.org/10.17509/ijost.v10i3.88934
p- ISSN 2528-1410 e- ISSN 2527-8045

[53] Kerans, G., Sanjaya, Y., Liliasari, L., Pamungkas, J., and Ate, Y. G. (2024). Effect of substrate and water on cultivation of Sumba seaworm (nyale) and experimental practicum design for improving critical and creative thinking skills of prospective science teacher in biology and supporting sustainable development goals (SDGs). *ASEAN Journal of Science and Engineering*, *4*(3), 383-404.

[54] Rahmat, A., Zahrani, A., Hidayat, H., Arum, F., Respati, S. A., Susanti, W. D., and Mutolib, A. (2025). Characteristics of jengkol peel (pithecellobium jiringa) biochar produced at various pyrolysis temperatures for enhanced agricultural waste management and supporting sustainable development goals (SDGs). *ASEAN Journal of Science and Engineering*, *5*(1), 145-172.

[55] Soegoto, H. S., Pohan, M. A. R., Luckyardi, S., Supatmi, S., Amasawa, E., Phithakkitnukoon, S., and Hasibuan, Z. A. (2025). Contributing factors to greenhouse gas emissions in agriculture for supporting sustainable development goals (SDGs): Insights from a systematic literature review completed by computational bibliometric analysis. *ASEAN Journal of Science and Engineering*, *5*(2), 199-230.

[56] Ab Rahman, M. H., Mahmud, J., Jumaidin, R., and Rahman, S. M. A. Integrated CRITIC-TOPSIS and Monte Carlo sensitivity analysis for optimal various natural fibre selection in sustainable building insulation composites to support the sustainable development goals (SDGs). *ASEAN Journal of Science and Engineering*, *5*(2), 231-260.

[57] Ragadhita, R., Fiandini, M., Nandiyanto, A. B. D., Septiani, E. L., Ogi, T., and Okuyama, K. Current strategies for mitigating airborne pathogen transmission: An integrative review based on aerosol science and particle technology to support the sustainable development goals (sdgs), complemented by a bibliometric analysis. *ASEAN Journal of Science and Engineering*, *5*(2), 261-314.

[58] Mukhamedov, G. I., Usarov, J. E., Khimmataliev, D. O., Komilov, K. U., Axmadjonov, D. B., Qorayev, S. B., and Rajabov, F. Development of interpolymer complexes for soil structure and water retention: a scientific and technological contribution to sustainable development goals (SDGs). *ASEAN Journal of Science and Engineering*, *5*(2), 315-326.

[59] Al Husaeni, D. N., and Haristiani, N. What evidence supports the advancement of language learning through digital innovation? Toward achieving sustainable development goals (sdgs) in the 21st century completed with bibliometric analysis. *ASEAN Journal of Science and Engineering*, *5*(2), 327-356.

[60] Prasetyo, I., Nugroho, A. A., Damayanto, A., and Fathoni, M. I. Developing an inclusive ict-based academic information system using rest api to promote sustainable development goals (sdgs) in higher education. *ASEAN Journal of Science and Engineering*, *5*(2), 395-416.

[61] Basnur, J., Putra, M. F. F., Jayusman, S. V. A., and Zulhilmi, Z. (2024). Sustainable packaging: Bioplastics as a low-carbon future step for the sustainable development goals (SDGs). *ASEAN Journal for Science and Engineering in Materials*, *3*(1), 51-58.

[62] Sesrita, A., Adri, H. T., Suherman, I., Rasmitadila, R., and Fanani, M. Z. (2025). Production of wet organic waste ecoenzymes as an alternative solution for environmental conservation supporting sustainable development goals (SDGs): A techno-economic and bibliometric analysis. *ASEAN Journal for Science and Engineering in Materials*, *4*(2), 245-266.

[63] Henny, H., Budi, A. H. S., Andriyansyah, M., Rozzak, M. R. A., Baru, M. M., and Masek, A. (2025). Hazard identification, risk assessment, and determining control (HIRADC) for workplace safety in manufacturing industry: A risk-control framework complete with

DOI: https://doi.org/10.17509/ijost.v10i3.88934
p- ISSN 2528-1410 e- ISSN 2527-8045

bibliometric literature review analysis to support sustainable development goals (SDGs). *ASEAN Journal for Science and Engineering in Materials*, *4*(2), 267-284.

[64] Syahrudin, D., Roestamy, M., Fauziah, R. S. P., Rahmawati, R., Pratidina, G., Purnamasari, I., and Salbiah, E. (2026). Techno-economic analysis of production ecobrick from plastic waste to support sustainable development goals (SDGs). *ASEAN Journal for Science and Engineering in Materials*, *5*(1), 9-16.

[65] Apriliani, A., Waahyudin, C., Ramdani, F. T., Martin, A. Y., Syahrudin, D., Hernawan, D., and Salbiah, E. (2026). Techno-economic analysis of sawdust-based trash cans and their contribution to indonesia's green tourism policy and the sustainable development goals (SDGs). *ASEAN Journal for Science and Engineering in Materials*, *5*(1), 17-36.

[66] Xing, G., Chano, J., Thadanatthaphak, Y., and Wu, C. C. (2025). Physical adaptation of college students in high-altitude training: Empirical findings and curriculum development insights to support sustainable development goals (sdgs). *ASEAN Journal of Educational Research and Technology*, *4*(2), 215-236.

[67] Imaniyati, N., Ratnasari, C. D., and Adman, A. (2025). Enhancing job satisfaction through human resource information systems and communication: A commitment-based approach to achieve sustainable development goals (sdgs) in education-oriented organizations. *ASEAN Journal of Educational Research and Technology*, *4*(2), 237-254.

[68] Maryanti, R., Rahayu, N. I., Muktiarni, M., Al Husaeni, D. F., Hufad, A.., Sunardi, S., and Nandiyanto, A. B. D. (2022). Sustainable development goals (SDGs) in science education: Definition, literature review, and bibliometric analysis. *Journal of Engineering Science and Technology*, *17*(6), 161-181.

[69] Fiandini, M., Nandiyanto, A. B. D., and Muktiarni, M. (2024). Experimental demonstration for teaching the concept of steam engine power plant to vocational students to support the sustainability development goals (sdgs) and its comparison to indonesian merdeka curriculum. *Journal of Engineering Science and Technology*, *19*(5), 1878-1905.

[70] Syahrul, S., Nurhayati, S., Wicaksono, M. F., and Fatimah, T. N. (2025). Internet of things-based child stunting detection system for supporting sustainable development goals. *Journal of Engineering Science and Technology*, *20*(2), 510-519.

[71] Suroto, S., Sundawa, D., and Prayoga Bestari, W. (2024). AppSheets on wetlands to realize sustainable development goals (SDGs). *Journal of Engineering Science and Technology (JESTEC)*, *19*(6), 97-104.

[72] Nandiyanto, A. B., Nugraha, A. Y., Fawwaz, L. T., Pramajati, M. F., Wijaya, Y. T., Fiandini, M. and Sukrawan, Y. (2025). Utilization of orange peel-derived biochar for ammonia adsorption: Isotherm analysis and hydrogen storage prospective for supporting sustainable development goals (SDGs). *Journal of Engineering Science and Technology*, *20*(1), 85-98.

[73] Supriatna, A., Tias, B., Hendayana, S., and Hernani, H. (2024). Global warming: Promoting environmental awareness of senior secondary school students facing issues in the sustainable development goals (Sdgs). *Journal of Engineering Science and Technology*, *19*(3), 1048-1064.

[74] Nandiyanto, A. B. D., Piantara, E., Alvani, C., Hafsah, D. W., Fathurohman, D., and Ragadhita, R. (2024). Fabrication of resin-based brake pad from snake fruit peel as sustainable renewable resources to support sustainable development goals (SDGs). *Journal of Engineering, Science and Technology*, *19*(5), 2022–2037.

[75] Nandiyanto, A. B. D., Ragadhita, R., Fiandini, M., Maryanti, R., Al Husaeni, D. N., and Al Husaeni, D. F. (2023). Adsorption isotherm characteristics of calcium carbon

DOI: https://doi.org/10.17509/ijost.v10i3.88934
p- ISSN 2528-1410 e- ISSN 2527-8045

microparticles prepared from chicken bone waste to support sustainable development goals (SDGs). *Journal of Engineering, Science and Technology*, *18*(2), 1363–1379.

[76] Nandiyanto, A. B. D., Al Husaeni, D. F., Ragadhita, R., Fiandini, M., Maryanti, R., and Al Husaeni, D. N. (2023). Computational calculation of adsorption isotherm characteristics of carbon microparticles prepared from mango seed waste to support sustainable development goals (SDGs). *Journal of Engineering, Science and Technology*, *18*(2), 913–930.

[77] Martin, A. Y., Roestamy, M., Qolyubi, A. T., Hakim, A. L., and Nandiyanto, A. B. D. (2024). Bibliometric analysis of the use of biochar in an environmental law perspective. *Journal of Engineering, Science and Technology*, *19*, 167–176.

[78] Anggraeni, S., Nandiyanto, A. B. D., and Usdiyana, D. (2023). Project effectivity of adsorbent from food waste for handling wastewater as a learning strategy to learning achievement of education for sustainable development and inquiry abilities. *Journal of Engineering, Science and Technology*, *18*(5), 2597–2614.

[79] Awa, A., Ramdani, F. T., Anwar, S.., Purnomo, A. M., Pengestu, R. A., Hutomo, Y. P., and Aziz, A. J. (2024). Production of pen holders from can waste for supporting sustainable development goals (SDGs): Technology and cost analysis. *Journal of Engineering Science and Technology*, *19*(6), 137-144.

[80] Ratmaningsih, N., Abdulkarim, A., Sopianingsih, P., Anggraini, D. N., Rahmat, R., Juhanaini, J., and Adhitama, F. Y. (2024). Gender equality education through augmented reality (AR)-based flashcards in learning social studies education in schools as an embodiment of sustainable development goals (SDGs). *Journal of Engineering Science and Technology*, *19*(4), 1365-1388.

[81] Vilmala, B. K., Suhandi, A., Permanasari, A., and Kaniawati, I. (2022). Profile (Knowledge, Attitude, and Practice) of sustainable science teacher at junior high schools in Riau towards the Sustainable Development Goals (SDGs). *Journal of Engineering Science and Technology*, *5*(2), 1-8.

[82] Nandiyanto, A. B. D., Putri, N. R., Firdaus, N. N., Anzety, N. D., Al'Hafsah, S. H., Yunatraya, S. A., and Sukrawan, Y. (2025). Red onion peel biomass carbon microparticles for ammonia adsorption for supporting hydrogen storage and sustainable development goals (SDGs) with isotherm analysis. *Journal of Engineering Science and Technology*, *20*(1), 181-194.

DOI: https://doi.org/10.17509/ijost.v10i3.88934
p- ISSN 2528-1410 e- ISSN 2527-8045